PHYSICAL REVIEW E **83**, 015101(R) (2011)

Stress concentration and size effect in fracture of notched heterogeneous material

Alexander S. Balankin, Orlando Susarrey, Carlos A. Mora Santos, Julián Patiño, Amalia Yoguez, and Edgar I. García
Grupo "Mecánica Fractal," Instituto Politécnico Nacional, México D.F., México 07738

(Received 12 October 2010; published 18 January 2011)

We study theoretically and experimentally the effect of long-range correlations in the material microstructure on the stress concentration in the vicinity of the notch tip. We find that while in a fractal continuum the notch-tip displacements obey the classic asymptotic for a linear elastic continuum, the power-law decay of notch-tip stresses is controlled by the long-range density correlations. The corresponding notch-size effect on fracture strength is in good agreement with the experimental tests performed on notched sheets of different kinds of paper. In particular, we find that there is no stress concentration if the fractal dimension of the fiber network is $D \leqslant d - 0.5$, where d is the topological dimension of the paper sheet.

DOI: 10.1103/PhysRevE.83.015101 PACS number(s): 46.50.+a, 62.20.mm, 81.40.Np

Understanding how materials fail is one of the most fundamental open problems in science and engineering (see Refs. [1–3] and references therein). In notched structures the fracture is controlled by material behavior around the notch tip [4]. A common approach to problems of crack initiation from a notch is based on linear elastic fracture mechanics (LEFM) [4,5]. Within the LEFM framework, it was shown that the displacement and stress fields ahead of a smooth notch scale with the distance from the notch tip r as $u_i = K_\alpha r^{1-\alpha_u} g_i(\alpha,\theta)$ and $\sigma_{ij} = K_\alpha r^{-\alpha_\sigma} f_{ij}(\alpha,\theta)$, respectively, where the scaling exponent $\alpha_u = \alpha_\sigma = \alpha$ plays a role similar to that of an eigenvalue and K_α is the generalized stress-intensity factor [5]. The value of α and the angular eigenfunctions $g_i(\alpha,\theta)$ and $f_{ij}(\alpha,\theta)$ can be determined by applying the traction-free boundary conditions to the notch flanks [4–6]. For a cut with smooth edges in a homogeneous elastic medium, it was found that $\alpha = 0.5$ and $K_{1/2}$ can be expressed in terms of the stress intensity factors for three standard loading modes, $K_{\rm I}$, $K_{\rm II}$, and $K_{\rm III}$ [5]. Therefore, the crack initiation criterion can be presented in the form $K_{1/2}(\sigma_{ij},a_0) = K_C$, where a_0 is the cut length and K_C is the apparent fracture toughness [4–6]. In a special case of the straight cut under loading mode I, the criterion of crack initiation is $K_I = \sigma_{22}\sqrt{2\pi a_0} = K_{IC}$, where K_{IC} is called the material toughness [4]. Accordingly, it is expected that the crack initiation stress σ_C scales with the notch size as $\sigma_C \propto K_{IC}/\sqrt{a_0}$, while K_{IC} is related to the critical value of the crack energy release rate G_C as $K_{IC} \propto \sqrt{G_C E}$, where E is the elastic modulus [6].

The heterogeneities in the microstructure of most real materials lead to inhomogeneous perturbations of the displacement and stress fields (see Refs. [7–11] and references therein). In particular, the heterogeneity introduces the disorder-dependent characteristic length l_C in the displacement and stress distributions [10,11]. As a result, the crack initiation stress is expected to scale with the cut size as

$$\sigma_C \propto \frac{K_C}{\sqrt{a_0 + l_C}} \tag{1}$$

for $a_0 > l_C$ [10]. So, in the large cut limit $a_0 \gg l_C$ the LEMF size effect law $\sigma_C \propto K_C/\sqrt{a_0}$ is recovered, where K_C is the disorder-dependent fracture toughness [10]. The size effect [Eq. (1)] was observed in experiments [10] and also reproduced in numerical simulations [10,11].

Once a crack is initiated, its motion is determined by balancing the energy that it dissipates with that which is externally supplied [12]. Rough crack paths in real materials do little resemble to smooth trajectories predicted in the classical LEFM [13]. Though, it was found that crack traces $z(x)$ often exhibit some kind of statistical scale invariance over a wide range of length scale, such that the height-height correlation function behaves as $C \propto (\Delta x)^{2\zeta}$, where ζ is the so-called roughness exponent [14–16]. It has been experimentally noted and then conjectured that cracks in materials with random microstructures are characterized by the universal roughness exponents $\zeta(d)$ (see Ref. [15] and references therein). This conjecture is consistent with the universality of critical exponents in percolation and other critical phenomena [17]. However, the situation can be changed drastically when there are long-range correlations in the heterogeneous microstructure. Specifically, in fibrous composites with power-law density correlations, the crack roughness exponent is a function of the fractal dimension of the microstructure [18]. Furthermore, some experiments with such materials suggest that the crack roughness exponent can be dependent on the fracture regime [19] and the crack orientation [20].

In this work, we study the effect of long-range density correlations on the stress concentration, crack roughness, and size effect in brittle fracture of notched paper sheets. Paper is a fiber composite material with many types of structural nonuniformities [21]. It was found that many types of commercial paper are characterized by a power-law behavior of the two-point density correlation function,

$$G(\vec{R}) = \langle [m(\vec{r}) - \overline{m}][m(\vec{r} + \vec{R}) - \overline{m}] \rangle \propto R^{-\eta}, \tag{2}$$

within a wide, but bounded, interval $l_0 < R < \xi$, where $m(\vec{r})$ is the local mass density, $\overline{m}$ is its average, $\langle \ldots \rangle$ is an average over the sheet, l_0 is the lower cutoff of the order of the average fiber size, and ξ is the structure-dependent correlation length [22]. For self-similar structures, such as fiber networks, the scaling exponent η is related to the fractal dimension D as $\eta = d - D$, where d is the embedding dimension [18,23]. Hence, at scale $l_0 < R < \xi$, the paper can be treated within a framework of the fractal continuum suggested in Ref. [24].

By using the concept of fractal continuum [24], the authors of Ref. [25] have shown that small strains in an elastic fractal

medium obeying the conventional constitutive law of linear elasticity, $\sigma_{ij} = \lambda\varepsilon_{kk}\delta_{ij} + 2\mu\varepsilon_{ij}$, should be defined as

$$\varepsilon_{ij} = 0.5[c_j(\partial u_i/\partial x_j) + c_i(\partial u_j/\partial x_i)], \tag{3}$$

where c_k's are the fractal functions ($k = 1,2,3$). For the fractal continuum considered in Ref. [24], the fractal functions have the form $c_k = \nu_k x_k^{\nu_k}$, where $\nu_k = D_{ij} + 1 - D$, while D_{ij} is the fractal dimension of surface in the (i,j) plane [26]. In the vicinity of a straight cut ($D_{ij} = d - 1$) in a linearly elastic heterogeneous medium, the displacements scale as $u_i \propto (r + l_C)^{1/2}$ [10]. If at scales $R > l_0 = l_C$ the medium obeys the fractal behavior characterized by Eq. (2), the fractal functions c_k can be represented in the form $c_k = \nu_k\,(x_k + l_0)^{d-D}$, and so the cut-tip strains defined by Eq. (3) and stresses $\sigma_{ij} = \lambda\varepsilon_{kk}\delta_{ij} + 2\mu\varepsilon_{ij}$ will behave as

$$\varepsilon_{ij} \propto \sigma_{ij} = K_\alpha\,(r + l_0)^{-\alpha_\sigma}\; f_{ij}(\alpha,\theta), \tag{4}$$

where the cut-tip stress exponent is

$$\alpha_\sigma = \frac{1 - 2(d - D)}{2}, \quad \text{if} \quad D \geqslant d - 1/2, \qquad \text{while } \alpha_\sigma = 0, \quad \text{if} \quad D \leqslant d - 1/2. \tag{5}$$

Accordingly, for a sheet with a straight cut of size $a_0 > l_0$ under loading mode I, the crack initiation stress is expected to obey the following size effect law,

$$\sigma_C \propto K_{MF}\,(a_0 + l_0)^{-\alpha_\sigma}\,, \tag{6}$$

where K_{MF} is the fractal material toughness. Notice that the fracture size effect law [Eq. (1)] is recovered from Eqs. (5) and (6) in the Euclidean limit $D = d$, e.g., for regular fiber networks and random networks with an exponential decay of $G(R)$, whereas, if $D \leqslant d - 1/2$, there is no the power-law stress concentration in the notch-tip vicinity, and so $\sigma_C = K_{MF} = \text{const}$ [27].

The paper toughness evaluation based on fracture mechanics has been extensively investigated by many scientists for the past two decades (see Ref. [28] and references therein). In many experimental works it was noted that the apparent toughness K_C obtained in tests of notched paper sheets is not a constant, but rather it is an increasing function of the notch size [29,30]. Furthermore, the analysis of the strain field in notched papers suggests that the notch-tip field cannot be described with stress intensity factor $K_{1/2}$ [31]. At the same time, the experimental data reported in Refs. [29,30], and [32] are consistent with the size effect [Eq. (6)] with $\alpha_\sigma < 0.5$. However, there are no dates on density correlations in papers tested in Refs. [29–32] and so, using $l_C = l_0$ and α as the fitting parameters, we can satisfactorily fit the same experimental data with either Eq. (1), or with Eqs. (5) and (6), over more than one decade of cut length scale [33].

To verify the size effect [Eqs. (5) and (6)], in this work we tested two types of paper with the known values of η. Specifically, we used the *Secante* paper of grade 200 ± 1 g/m^2 and the *Filtro* paper of grade 103.4 ± 0.9 g/m^2. Earlier, both papers were used in Ref. [18] for the study of damage fractures in sheets without notches. It was found that for both papers the two-point density correlation function obeys the scaling behavior (2) with $l_0 = 1.8$ mm and $\eta = 0.37 \pm 0.03$ for *Secante* paper, while it was $l_0 = 1.15$ mm and $\eta = 0.51 \pm 0.05$

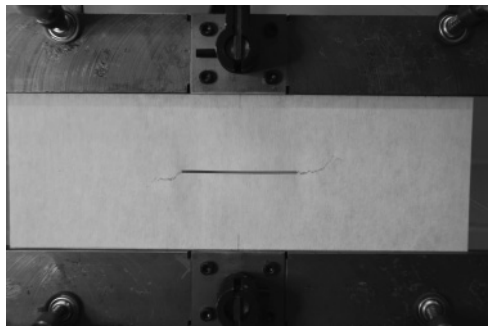

FIG. 1. Snapshot of stable crack propagation in the notched sheet of the *Filtro* paper of width $W = 300$ mm and $a_0/W = 0.25$.

for *Filtro* paper [18]. In this work, we tested the center notched sheets of length 200 mm (the working length is 110 mm), while the sheet width $W = \lambda W_0$ was varied within the interval $10 = W_0 \leqslant W \leqslant 400$ mm with scale factors of $\lambda = 1$, 2.5, 5, 10, 15, 20, 25, 30, 35, 40. The initial cuts in the sheets were made by a scalpel [34]. Three series of tests were performed in specimens with different ratios of the cut length to the sheet width, $\mu = a_0/W$. First, the crack initiation tests were performed in specimens with the fixed ratio $\mu = 0.25$. Additionally, we tested the notched *Filtro* paper sheets of width 300 and 400 mm with different ratios μ in the range of $0.025 \leqslant \mu \leqslant 0.375$. In addition, the sheets without notches were tested to determine the tensile strength σ_t of each paper. Mechanical tests were carried out on a mechanical testing system (MTS) 858-5 testing machine. The sheets were held by pneumatic vise-action grips between two parallel textured jaw faces (see Fig. 1). At least ten identical specimens of each size were tested under the same loading conditions [35]. In all experiments, the crack initiation was determined from *in situ* observations with an optical microscope. In some experiments, crack propagation through the specimen was monitored through the use of a video recording system. Both papers obey elastoplastic behavior (see Fig. 2) and the failure of sheets without notches is governed by the damage mechanics (see Ref. [18]). However, we noted that the crack initiation stresses (σ_C) in the notched sheets of these papers are less than

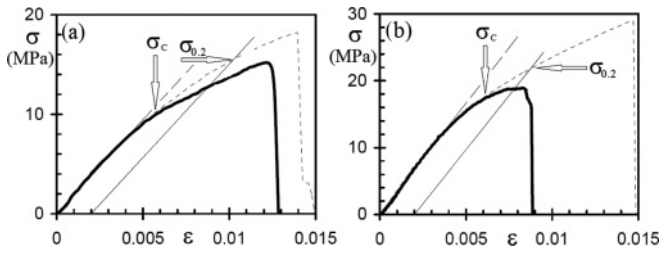

FIG. 2. Stress-strain curves for the sheets of (a) *Secante* and (b) *Filtro* papers without (dashed curve) and with (solid curve) a central cut. The arrows indicate the paper yield stresses $\sigma_{0.2}$ (defined as the stress at which a plastic deformation achieves 0.2%) and the crack initiation stresses σ_C determined from observation with an optical microscope in notched sheets of width $W = 400$ mm and $a_0/W = 0.25$. Notice that for sheets with notches the stress is defined as $\sigma = F/h(W - a_0)$, where F is the applied tensile force and h is the sheet thickness.

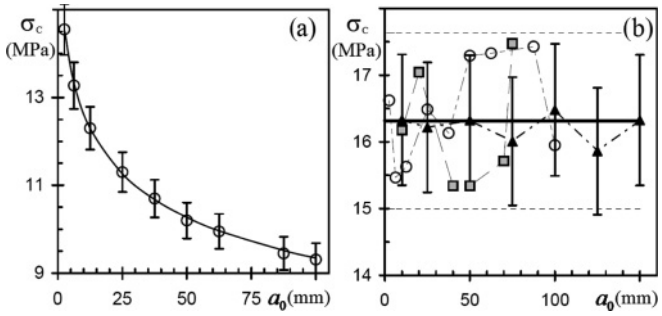

FIG. 3. Crack initiation stress σ_C vs cut length a_0 in sheets of (a) *Secante* and (b) *Filtro* papers. Symbols: experimental data for sheets with $a_0/W = 0.25$ (circles) and for sheets of width $W =$ 400 mm (triangles) and $W = 300$ mm (squares); notice that each experimental point is the average over ten experiments, while error bars denote the statistical error calculated as $\pm 2s(\sigma_C)$, where $s(\sigma_C)$ is the standard deviation of ten measurements [for clarity in (b), error bars are shown for one series of tests only]. Solid curve in (a): data fitting by Eq. (6) with $l_0 = 1.8$ mm, $\alpha = 0.14$, and $K_{MF} = 6.78\,\text{MPa m}^{0.14}$. In (b) the solid line represents the mean value $\sigma_C = 16.3$ MPa, while dashed lines show the interval of confidence at 95%.

their yield stresses ($\sigma_{0.2}$) such that the crack propagation is brittle.

The log-log plots of the crack initiation stress σ_C versus the cut length a_0 in sheets with a ratio $a_0/W = 0.25$ are shown in Figs. 3(a) and 3(b). The data for the *Secante* paper obey the size scaling law shown in Eq. (6) with the scaling exponent $\alpha = 0.14 \pm 0.02$ [see Fig. 3(a)], which is consistent with Eq. (5). Therefore, the crack initiation criterion can be presented in the form $K_\alpha = \sigma\,(a_0 + l_0)^{0.14} = K_{MF}$, where the fractal material toughness of *Secante* paper is $K_{MF} = \sigma_C a_0^{0.14} = 6.78 \pm 0.07\,\text{MPa m}^{0.14}$. In contrast to this, the crack initiation stress in the *Filtro* paper is found to be independent on the crack length in the range of $5 \leqslant a_0 \leqslant 150$ mm, as well as on the ratio a_0/W in the range of $0.025 \leqslant a_0/W \leqslant 0.375$ [see Fig. 3(b)]. This is consistent with the prediction of the size effect law [Eq. (6)] with $\alpha_\sigma = 0$ expected from Eq. (5). The difference between the crack initiation stress, $\sigma_C = K_{MF} = 16.3 \pm 1.3$ MPa, and the maximal tensile strength of the *Filtro* papersheets without notches, $\sigma_t = 28 \pm 3$ MPa [see Fig. 1(b)], can be attributed to the difference in the fracture mechanisms of sheets with and without the initial notch. In fact, sheets without notches fail owing to damage accumulation (see Ref. [18]), whereas the fracture of notched sheets is owing to single crack propagation. It should be pointed out that the independence of crack initiation stress within a wide range of the cut length $a_0 > l_0 \approx l_C$ cannot be explained with the size effect law defined by Eq. (1) [29].

Once stated, the crack follows an irregular path, reflecting certain constituents of paper microstructure and stress fluctuations. To study crack roughness, all fractured sheets were scanned with a 1200 ppp resolution and then the crack traces were digitized with the help of Scion Image software (see Ref. [36]). The crack roughness exponents of digitized crack traces were determined by the variogram, power spectrum, roughness length, and rescaled range (R/S) methods with the help of the BENOIT 1.3 software (see Refs. [18] and [37]). In this way we found that the roughness of cracks in the *Secante* and *Filtro* papers is characterized by the local roughness exponents $\zeta = 0.64 \pm 0.03$ and $\zeta = 0.49 \pm 0.01$, respectively. We noted that these values are statistically indistinguishable from the roughness exponents of damage fractures obtained in tensile tests of sheets without notches (see Ref. [18]). In Ref. [18], it was shown that the damage fracture roughness exponent is related to the fractal dimension of the fiber network as $\zeta = D - (d - 1)$. Our findings suggest that the roughness exponents of brittle cracks in the *Secante* and *Filtro* papers also obey this relation [38].

In summary, we showed that in a fractal continuum the distribution of notch-tip stresses is controlled by the long-range density correlations. This is reflected in the notch-size effect on the crack initiation stress [Eqs. (5) and (6)]. The scale invariant density fluctuations also determine the scaling properties of crack roughness. These findings provide a novel insight into the fracture phenomena in materials with a fractal microstructure.

This work was partially supported by the FONCICYT (México–European Union) under Project 96095 and the Government of Mexico City under Grant No. PICCT08-64.

[1] L. Ponson, Phys. Rev. Lett. **103**, 055501 (2009); J. Scheibert, C. Guerra, F. Célarié, D. Dalmas, and D. Bonamy, *ibid.* **104**, 045501 (2010); S. S. Chakravarthy and W. A. Curtin, *ibid.* **105**, 115502 (2010).

[2] E. Bouchbinder and T.-Sh. Lo, Phys. Rev. E **78**, 056105 (2008); J. A. Åström, *ibid.* **80**, 046113 (2009); Y. Cohen and I. Procaccia, *ibid.* **81**, 066103 (2010); E. Bouchbinder, *ibid.* **82**, 015101(R) (2010).

[3] G. P. Cherepanov, A. S. Balankin, and V. S. Ivanova, Eng. Fract. Mech. **51**, 997 (1995); B. Cotterell, *ibid.* **69**, 533 (2002); Z. P. Bazant and A. Yavari, *ibid.* **72**, 1 (2005); F. M. Borodich, J. Mech. Phys. Solids **45**, 239 (1997); M. J. Alava, P. K. V. V. Nukala, and S. Zapperi, Adv. Phys. **55**, 349 (2006); S. Pradhan, A. Hansen, and B. K. Chakrabarti, Rev. Mod. Phys. **82**, 499 (2010).

[4] K. B. Broberg, *Cracks and Fracture* (Academic Press, New York, 1999).

[5] A. Seweryn and K. Molski, Eng. Fract. Mech. **55**, 529 (1996); D. Leguillon and Z. Yosibash, Int. J. Fract. **122**, 1 (2003); P. Lazzarin and S. Filippi, Int. J. Solids Struct. **43**, 2461 (2006); M. P. Savruk and A. Kazberuk, Int. J. Fract. **161**, 79 (2010).

[6] J. R. Willis, Int. J. Fract. **100**, 85 (1999); A. S. Balankin, Eng. Fract. Mech. **57**, 135 (1997); M. P. Wnuk and A. Yavari, *ibid.* **76**, 548 (2009); A. Carpinteri and M. Paggi, *ibid.* **76**, 1771 (2009).

[7] I. L. Menezes-Sobrinho, A. T. Bernardes, and J. G. Moreira, Phys. Rev. E **63**, 025104(R) (2001); S. Santucci, L. Vanel, and S. Ciliberto, Phys. Rev. Lett. **93**, 095505 (2004); I. Malakhovsky and M. A. J. Michels, Phys. Rev. B **76**, 144201 (2007).

[8] A. S. Balankin, O. Susarrey, and A. Bravo, Phys. Rev. E **64**, 066131 (2001).

[9] F. Barra, A. Levermann, and I. Procaccia, Phys. Rev. E **66**, 066122 (2002).

[10] M. J. Alava, P. K. V. V. Nukala, and S. Zapperi, Phys. Rev. Lett. **100**, 055502 (2008); J. Phys. D **42**, 214012 (2009).

[11] Ch. Urabe and Sh. Takesue, Phys. Rev. E **82**, 016106 (2010).

[12] T. Goldman, A. Livne, and J. Fineberg, Phys. Rev. Lett. **104**, 114301 (2010).

[13] V. Y. Milman, N. A. Stelmashenko, and R. Blumenfeld, Prog. Mater. Sci. **38**, 425 (1994); A. S. Balankin and F. J. Sandoval, Rev. Mex. Fis. **43**, 545 (1997); P. Kotowski, Int. J. Fract. **141**, 269 (2006); S. Santucci, K. Jørgen Måløy, A. Delaplace, J. Mathiesen, A. Hansen, J. O. H. Bakke, J. Schmittbuhl, L. Vanel, and P. Ray, Phys. Rev. E **75**, 016104 (2007); D. Bonamy, J. Phys. D **42**, 214014 (2009).

[14] P. Meakin, *Fractals, Scaling and Growth far from Equilibrium* (Cambridge University Press, New York, 1998).

[15] E. Bouchaud, G. Lapasset, and J. Planes, Europhys. Lett. **13**, 73 (1990); E. Bouchaud, J. Phys. Condens. Matter **9**, 4319 (1997); L. Ponson, D. Bonamy, and E. Bouchaud, Phys. Rev. Lett. **96**, 035506 (2006).

[16] A. S. Balankin and O. Susarrey, Int. J. Fract. **81**, R27 (1996); **87**, R37 (1997); Philos. Mag. Lett. **79**, 629 (1999); A. S. Balankin, D. M. Matamoros, and I. Campos, *ibid.* **80**, 165 (2000); A. S. Balankin, O. Susarrey, R. García Paredes, L. Morales, D. Samayoa, and J. A. López, Phys. Rev. E **72**, 065101 (2005).

[17] A. Hansen and J. Schmittbuhl, Phys. Rev. Lett. **90**, 045504 (2003).

[18] A. S. Balankin, O. Susarrey, and J. M. Gonzáles, Phys. Rev. Lett. **90**, 096101 (2003).

[19] N. Mallick, P.-P. Cortet, S. Santucci, S. G. Roux, and L. Vanel, Phys. Rev. Lett. **98**, 255502 (2007).

[20] I. L. Menezes-Sobrinho, M. S. Couto, and I. R. B. Ribeiro, Phys. Rev. E **71**, 066121 (2005).

[21] M. Alava and K. Niskanen, Rep. Prog. Phys. **69**, 669 (2006).

[22] N. Provatas, M. J. Alava, and T. Ala-Nissila, Phys. Rev. E **54**, R36 (1996).

[23] E. Sharon, M. G. Moore, W. D. McCormick, and H. L. Swinney, Phys. Rev. Lett. **91**, 205504 (2003).

[24] V. E. Tarasov, Phys. Lett. A **336**, 167 (2005).

[25] J. Li and M. Ostoja-Starzewski, Proc. R. Soc. London, Ser. A **465**, 2521 (2009).

[26] M. Ostoja-Starzewski, Acta Mech. **205**, 161 (2009).

[27] Notice that at scales larger than ξ the fractal correlations [Eq. (2)] vanish and the material is characterized by $D = d$. Hence, in the large cut limit $a_0 \gg \xi$, the size effect law [Eqs. (5) and (6)] transforms in the size effect law [Eq. (1)] with $l_C = \xi \gg l_0$ and the crack initiation is controlled by the disorder-dependent fracture toughness K_C.

[28] T. Yamauchi and H. Hirano, J. Wood Sci. **46**, 79 (2000); J. Tryding and P. J Gustafsson, J. Pulp Pap. Sci. **27**, 103 (2001); W. J. Batchelor and D. M. S. Wanigaratne, Int. J. Fract. **123**, 15 (2003).

[29] G. Sinclair, M. Kondo, and R. Pieri, Int. J. Fract. **72**, R3 (1995); A. S. Balankin *et al.*, *ibid.* **79**, R63 (1996); **90**, L57 (1998).

[30] A. S. Balankin, Int. J. Fract. **76**, R63 (1996); A. S. Balankin *et al.*, *ibid.* **79**, R63 (1996); **90**, L57 (1998).

[31] G. J. Dvorak and A. P. Suvorov, Int. J. Fract. **95**, 89 (1999); P. Isaksson and R. Hägglund, Int. J. Solids Struct. **44**, 659 (2007).

[32] A. S. Balankin, L. H. Hernandez, G. Urriolagoitia, O. Susarrey, J. M. Gonzáles, and J. M. Trinidad, Proc. R. Soc. London, Ser. A **455**, 2565 (1999).

[33] Originally, in Refs. [30] and [32], the size effect of the form Eq.(6) with $l_C/a_0 = 0$ and $\alpha_\sigma < 0.5$ has been attributed to the crack roughness, nonetheless that crack initiation stress was measured in sheets with straight cuts. While the possible effect of the fractal structure of paper was also pointed in Ref. [32], the corresponding relation (1.4) from Ref. [32] differs from Eq. (5). To verify scaling relations [Eq. (6)] together with Eq. (5) experimentally, we need to test materials with known D and $a_0 \gg l_0$. In this way, the most clear difference between predictions with scaling laws [Eq. (1)] and [Eqs. (5) and (6)] is expected for materials with $D \leqslant d - 1/2$.

[34] Both papers have a well-defined anisotropy of mechanical properties associated with preferable orientation of fibers in the machine direction (see Ref. [18]). Accordingly, in this work, all cuts were made perpendicular to the machine direction. The notch-curvature radius is of the order of the fiber width $w \ll l_0$.

[35] All tests were made with the grip displacement speed of 1 mm/min at a relative humidity of 50 $\pm$ 3% and a temperature of 23$\pm$2 °C.

[36] [http://www.sciocorp.com] (Scion-Image, 2010).

[37] [http://www.trusoft-international.com] (BENOIT 1.3, 2009); W. Seffens, Science **285**, 1228 (1999).

[38] It is possible that a more fine scaling analysis, e.g., such as performed in Ref. [17], will permit to distinguish between the scaling properties of damage and brittle cracks, but this is not the subject of the present Rapid Communication.